

# Dielectric, magnetic, and magnetoelectric properties of La and Ti codoped BiFeO<sub>3</sub>

Y. F. Cui,<sup>1</sup> Y. G. Zhao,<sup>1,a)</sup> L. B. Luo,<sup>1</sup> J. J. Yang,<sup>1</sup> H. Chang,<sup>1</sup> M. H. Zhu,<sup>1</sup> D. Xie,<sup>2</sup> and T. L. Ren<sup>2</sup>

<sup>1</sup>Department of Physics, Tsinghua University, Beijing 100084, China

<sup>2</sup>Tsinghua National Laboratory for Information Science and Technology (TNList) and Institute of Microelectronics, Tsinghua University, Beijing 100084, China

(Received 22 August 2010; accepted 13 November 2010; published online 3 December 2010)

The authors report on the dielectric, magnetic, and magnetoelectric (ME) properties of La and Ti codoped BiFeO<sub>3</sub> (LBFTO). Codoping changes the structure of BiFeO<sub>3</sub> from rhombohedral to tetragonal and the ferromagnetic properties of LBFTO are remarkably improved. More interestingly, the dielectric constant of LBFTO shows a linear increase with magnetic field and the slope decreases linearly with increasing temperature. The electric polarization of LBFTO also increases upon applying a magnetic field. The ME coupling coefficients of different orders were obtained by analyzing these data. The results were discussed by considering the doping induced destruction of the cycloidal structure in LBFTO. © 2010 American Institute of Physics. [doi:10.1063/1.3524225]

BiFeO<sub>3</sub> (BFO) is the few one among the multiferroic materials with the ferroelectric and magnetic orders above room temperature.<sup>1</sup> BFO possesses a distorted perovskite structure with the space group *R3c*, an antiferromagnetic Néel temperature of 370 °C, and a ferroelectric Curie temperature of 830 °C.<sup>2</sup> In BFO, along the threefold pseudocubic [111]<sub>c</sub> rotation axis, the Bi<sup>3+</sup> and Fe<sup>3+</sup> cations are displaced from their centrosymmetric positions, leading to a spontaneous polarization. As a result, the inversion center is absent in BFO. In this case, BFO can simultaneously possess weak ferromagnetism and a linear magnetoelectric (ME) effect, which are forbidden in the antiferromagnets with an inversion center in their structures.<sup>3</sup> The linear ME effect corresponds to the induction of polarization by a magnetic field or magnetization by an electric field with a linear field dependence.<sup>4</sup> It is supplemented by the higher-order ME effects.<sup>4</sup> The magnetic moments of Fe<sup>3+</sup> cations in BFO couple ferromagnetically within the pseudocubic (111) planes and antiferromagnetically between the adjacent planes showing the G-type antiferromagnetic order. However, it has been shown that a long-range incommensurate cycloidal spiral magnetic structure with a large period of 62 nm is present in BFO.<sup>5</sup> This cycloidal structure results in the disappearance of the weak ferromagnetism and the linear ME effect due to the averaging over the period. It has been shown that both high magnetic field (20 T) (Ref. 6) and doping can suppress the cycloidal structure of BFO and release the weak ferromagnetism and linear ME effect.<sup>3</sup> So doping is an effective way to suppress the cycloidal structure of BFO. Moreover, doping can also dramatically reduce the leakage current and improve the magnetic properties of BFO.<sup>7–16</sup> For example, La doping at Bi site enhances the ferromagnetic property of BFO,<sup>10</sup> while Ti doping at Fe site reduces the leakage current of BFO.<sup>9</sup> So, it is interesting to explore the effect of codoping of La and Ti on BFO in order to combine the advantages of La doping and Ti doping. The ME effect in the doped BFO with the suppression of the cycloidal structure is also an interesting topic. So far, there are only a few reports on the codoping effect of La and Ti in BFO, focusing on the elec-

tronic transport mechanism, ferroelectric, and impedance behavior.<sup>14,15</sup> Moreover, the study of ME coupling in the doped BFO combining both the dielectric constant measurement and the electric polarization measurement is still lacking. In this letter, we report on the effect of La and Ti codoping on the dielectric, magnetic, and ME properties of BFO.

Bi<sub>0.85</sub>La<sub>0.15</sub>Fe<sub>0.9</sub>Ti<sub>0.1</sub>O<sub>3</sub> (LBFTO) samples were prepared by the rapid liquid phase sintering method.<sup>17</sup> High purity powders of La<sub>2</sub>O<sub>3</sub>, Bi<sub>2</sub>O<sub>3</sub>, Fe<sub>2</sub>O<sub>3</sub>, and TiO<sub>2</sub> were used as the starting materials. These materials were carefully weighed in stoichiometric proportion, dried at 300 °C for 2 h. Then the samples were ground and pressed into pellets with a 12 mm diameter and 1 mm thickness. The pellets were then heated to 900 °C with a heating rate of 100 °C/s and kept at 900 °C for 2 h. After sintering, the samples were quenched to room temperature. For comparison, Bi<sub>0.85</sub>La<sub>0.15</sub>FeO<sub>3</sub> (LBFO) and BiFe<sub>0.9</sub>Ti<sub>0.1</sub>O<sub>3</sub> (BFTO) samples were also prepared with the same conditions. The phase of the samples was characterized by x-ray diffraction (XRD) (Rigaku diffractometer with nickel filtered Cu K $\alpha$  radiation). Dielectric property was measured by using a LCR meter. Au electrodes were prepared by magnetron sputtering. A superconducting quantum interference device magnetometer (MPMS XL7) was used for measuring the magnetic field and temperature dependence of the magnetization and dielectric constants of the samples. The effect of magnetic field on polarization was measured by using a Keithley 6517A electrometer.

Figure 1(a) is the XRD patterns of LBFTO, LBFO, and BFTO, which indicates that all samples are single phase. The existence of splitting peaks around 31° and 39° for LBFO and BFTO suggests the distorted rhombohedral *R3c* structure, which is consistent with those reported by other groups.<sup>10,13,16</sup> For the La and Ti codoped samples, the splitting of diffraction peaks around 22° and 45° suggests a phase transition from rhombohedral to tetragonal, which has been reported in the La, Nd, or Ba doped bulk BFO.<sup>7,8,11</sup> Figures 1(b)–1(d) show the scanning electron microscopy (SEM) images of the samples. It can be seen that doping does not lead to obvious change in grain size and morphology.

The magnetic hysteresis loops for LBFTO, LBFO, and BFTO are presented in Fig. 2. The magnetization curves are

<sup>a)</sup>Electronic mail: ygzhao@tsinghua.edu.cn.

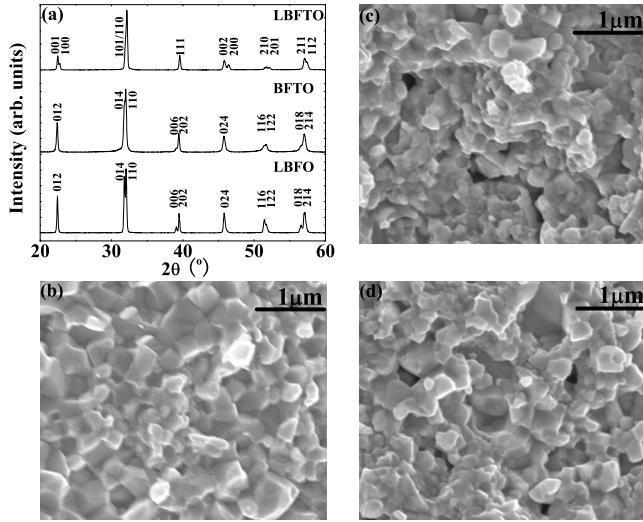


FIG. 1. (a) XRD patterns for LBFO, BFTO, and LBFTO. [(b)–(d)] The SEM images of LBFO, BFTO, and LBFTO.

not saturated in the fields up to 70 kOe. Compared with LBFO and BFTO, there is an obvious enhanced magnetization for LBFTO samples. BFO is known to be antiferromagnetic with a G-type magnetic structure, but has a residual magnetic moment due to a canted spin structure,<sup>3</sup> and the G-type structure is modified by the long-range modulation of the cycloidal spiral with the [110] spiral direction and (1 $\bar{1}$ 0) spin rotation plane.<sup>5</sup> This cycloidal structure results in the disappearance of the weak ferromagnetism due to the averaging over the period. As shown in Fig. 1, La and Ti codoping can induce the structural transition from rhombohedral to tetragonal which destroys the cycloidal spin structure and results in a homogeneous spin structure.<sup>7,11,12</sup> So the latent magnetization locked within the cycloid is released. This can account for the remarkable enhancement of magnetization for LBFTO compared with LBFO and BFTO.

Figures 3(a) and 3(b) show the dielectric constant and dielectric loss as a function of temperature for LBFTO, LBFO, and BFTO, respectively. At higher temperatures (220–300 K) the dielectric constant for LBFO increases remarkably, presumably due to the Maxwell–Wagner-type contribution to the dielectric constant.<sup>18</sup> In contrast, this behavior was not observed in BFTO and LBFTO samples. The frequency dependences of dielectric constant and dielectric loss for LBFTO, LBFO, and BFTO are shown in Figs. 3(c) and 3(d). For LBFO, the dielectric constant with a large

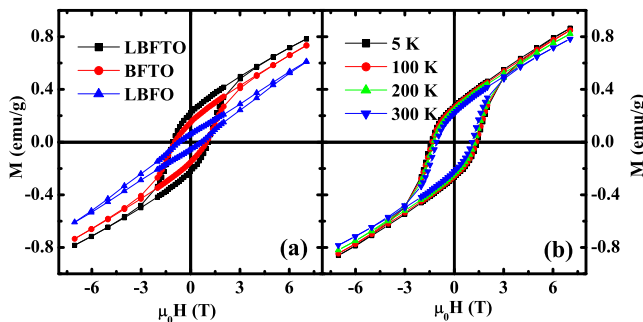


FIG. 2. (Color online) (a) Magnetic hysteresis loops for LBFO, BFTO, and LBFTO at room temperature. (b) Magnetic hysteresis loops for LBFTO at different temperatures.

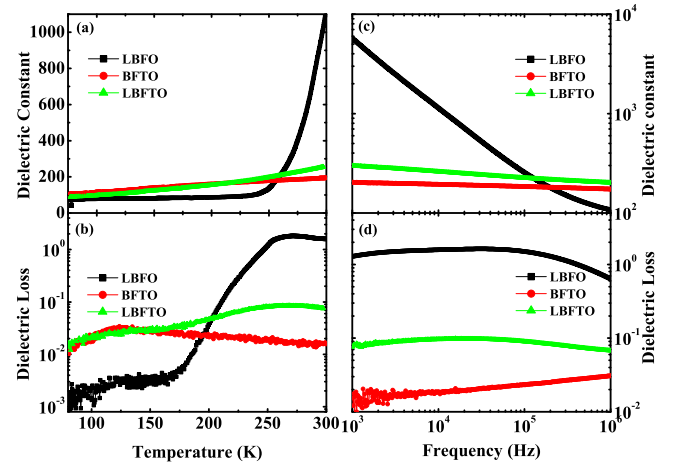


FIG. 3. (Color online) (a) Temperature dependence of dielectric constant and (b) dielectric loss for LBFO, BFTO, and LBFTO measured at 10 kHz. (c) Frequency dependence of dielectric constant and (d) dielectric loss for LBFO, BFTO, and LBFTO measured at room temperature.

value at low frequencies decreases with increasing frequency and is nearly constant at high frequencies. This phenomenon can be attributed to the Maxwell–Wagner-type contribution to the dielectric constant, which is also present in the temperature dependence of dielectric constant for LBFO. This phenomenon is related to the space charge relaxation at the interface. The space charges are suggested to originate from  $V_{O}^{2+}$ ,  $V_{Bi}^{3-}$ , etc. At low frequencies, the space charges can follow the applied electric field and contribute to the dielectric constant. While at high frequencies, they do not have time to build up and undergo relaxation. Compared to LBFO, the substitution of  $Ti^{4+}$  for  $Fe^{3+}$  in LBFTO reduces the oxygen vacancies significantly because of the requirements of charge compensation, leading to the absence of the Maxwell–Wagner effect. The frequency dependence of dielectric constant for LBFTO is weaker than that of LBFO and the dielectric loss of LBFTO is smaller than that of LBFO.

In order to study the ME effect in LBFTO samples, we measured the magnetic field dependence for the dielectric constant at different temperatures. The dielectric constant was measured at frequencies of 10 and 180 kHz, respectively, and it does not change with frequency. As shown in Fig. 4(a), the relative change of dielectric constant of LBFTO, defined by  $[\varepsilon(H)-\varepsilon(0)]/\varepsilon(0)$ , shows a roughly linear dependence on magnetic field at all temperatures, which is consistent with the destruction of the cycloidal structure of BFO and the resultant release of the linear ME effect. It can be seen from Fig. 4(a) that the slope of  $[\varepsilon(H)-\varepsilon(0)]/\varepsilon(0)$  versus  $H$  increases with decreasing temperature and this behavior was plotted in Fig. 4(b). For comparison, the temperature dependence of  $1/\varepsilon(0)$  was also shown in Fig. 4(b) and it shows a correlation with the  $[\varepsilon(H)-\varepsilon(0)]/\varepsilon(0)\Delta H$ . So it can be deduced that the temperature dependence of  $[\varepsilon(H)-\varepsilon(0)]/\varepsilon(0)\Delta H$  originates from the temperature dependence of  $1/\varepsilon(0)$ . Thus,  $\varepsilon(H)-\varepsilon(0)$  is independent on temperature. For materials showing ME effect, the electric polarization is determined by the following formula:<sup>4</sup>

$$P_i(\vec{E}, \vec{H}) = -\frac{\partial F}{\partial E_i} = P_i^S + \varepsilon_0 \varepsilon_{ij} E_j + \alpha_{ij} H_j + \frac{1}{2} \beta_{ijk} H_j H_k + \gamma_{ijk} H_j E_k - \dots, \quad (1)$$

where  $P_i^S$  is the spontaneous polarization, and  $E$  and  $H$  are

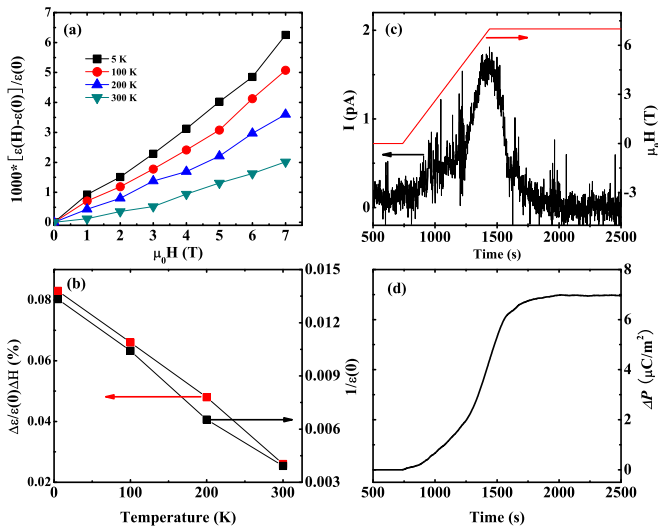


FIG. 4. (Color online) (a) Magnetic field-induced relative change of the dielectric constant for LBFTO at different temperatures. (b) Correlation of  $[\varepsilon(H)-\varepsilon(0)]/\varepsilon(0)\Delta H$  with  $1/\varepsilon(0)$ . (c) The application of magnetic field from 0 to 7 T and the polarization change induced discharge current measured at 5 K. (d) The polarization change upon application of magnetic field obtained from (c) by integral of current with time.

the applied electric and magnetic fields, respectively.  $\varepsilon_0$  is the free space permittivity and  $\varepsilon_{ij}$  is the relative permittivity tensor.  $\alpha_{ij}$ ,  $\beta_{ijk}$ , and  $\gamma_{ijk}$  are the ME coupling coefficients of different orders. For the undoped BFO, the cycloidal spiral magnetic structure (Ref. 5) results in the average of antiferromagnetic vector  $L$  to be zero. Since both  $\alpha$  and  $\gamma$  are proportional to  $L$ , the average of  $\alpha$  and  $\gamma$  is also zero for the undoped BFO (Ref. 16) resulting in the absence of the linear ME effect. So the linear  $H$  dependences of polarization and dielectric constant have not been observed in the undoped BFO. For LBFTO, in contrast, the destruction of cycloidal spiral magnetic structure allows one to measure the linear ME effect, and get the ME coupling coefficient of  $\alpha$  and  $\gamma$  by the measurements of the dielectric constant and electric polarization, respectively. It has been reported that the magnetic field dependent dielectric constant tensor  $\varepsilon_{ij}(H)$  obtained by ac measurement is determined by  $\varepsilon_{ij}(0) + \frac{1}{2}\gamma_{kij}H_k$ , where the ME coupling coefficient  $\gamma_{kij}$  depends linearly on the antiferromagnetic vector  $L$  of BFO.<sup>16</sup> For the polycrystalline samples as in our work, the dielectric constant is averaged and it can be simply expressed as  $\varepsilon(H) = \varepsilon(0) + \frac{1}{2}\gamma H$ . Based on this formula, the independence of  $\varepsilon(H) - \varepsilon(0)$  on temperature reflects that the ME coupling coefficient  $\gamma$  or the antiferromagnetic vector  $L$  of LBFTO does not change with temperature. Using the data in Fig. 4(a), the ME coupling coefficient  $\gamma$  was calculated to be  $(1.30 \pm 0.11) \times 10^{-18}$  s/V. It should be mentioned that the value of  $\gamma$  for the doped BFO has not been reported before. To further explore the ME effect in LBFTO and get the average value of the ME coupling coefficient  $\alpha$ , we measured the change of the electric polarization  $P$  upon application of a magnetic field. A voltage of 400 V was applied on the sample (0.1 mm thick) at 400 K and then the sample was cooled down from 400 to 5 K. The voltage was removed at 5 K. After enough time for stabilization, a magnetic field was applied from 0 to 7 T and the polarization change induced magnetoelectric cur-

rent was measured and the result is shown in Fig. 4(c). The polarization change ( $\Delta P$ ) is shown in Fig. 4(d), which was obtained by the integral of current with time. The polarization change ( $\Delta P$ ) is shown in Fig. 4(d), which was obtained by the integral of current with time. The polarization change at 7 T is  $7 \mu\text{C}/\text{m}^2$ . According to formula (1), the average value of ME coupling coefficient  $\alpha$  was obtained to be  $(1.01 \pm 0.14) \times 10^{-10} \text{ C m}^{-2} \text{ Oe}^{-1}$  since  $\Delta P \approx \alpha H$ . This value is closed to that reported in BFO whose cycloidal spiral magnetic structure was destroyed by a high magnetic field with the resultant releases of the linear ME effect.<sup>3</sup>

For the magnetodielectric in BFO, it is important to rule out the extrinsic effect. It has been proposed by Catalan that a combination of magnetoresistance and Maxwell–Wagner effect can result in the magnetodielectric effect.<sup>19</sup> The main behaviors involving this mechanism are as follows. First, with increasing temperature, a dramatic increase of dielectric constant occurs at a certain temperature, manifesting the occurrence of the Maxwell–Wagner effect.<sup>18</sup> Second, the magnetodielectric effect is remarkable only in the temperature range that the Maxwell–Wagner effect occurs.<sup>18</sup> As shown in Fig. 3(a), the dielectric constant of LBFTO does not show a dramatic increase with increasing temperature indicating the absence of the Maxwell–Wagner effect in this temperature range. More importantly, the magnetodielectric effect becomes more remarkable at low temperatures [Fig. 4(a)], which can not be explained by the combination of magnetoresistance and Maxwell–Wagner effect.

This work was supported by the 973 project (Grant No. 2009CB929202), the National Science Foundation of China (Grant No. 50872065), the Tsinghua National Laboratory for Information Science and Technology (TNList) Cross-discipline Foundation, and the Specialized Research for the Doctoral Program of Higher Education.

- <sup>1</sup>G. Catalan and J. F. Scott, *Adv. Mater. (Weinheim, Ger.)* **21**, 2463 (2009).
- <sup>2</sup>V. G. Bhide and M. S. Multani, *Solid State Commun.* **3**, 271 (1965).
- <sup>3</sup>A. M. Kadomtseva, A. K. Zvezdin, Yu. F. Popov, A. P. Pyatakov, and G. P. Vorob'ev, *JETP Lett.* **79**, 571 (2004).
- <sup>4</sup>M. Fiebig, *J. Phys. D* **38**, R123 (2005).
- <sup>5</sup>I. Sosnowska, T. P. Neumaier, and E. Steichele, *J. Phys. C* **15**, 4835 (1982).
- <sup>6</sup>Yu. F. Popov, A. Zvezdin, G. Vorob'ev, A. Kadomtseva, V. Murashev, and D. Rakov, *JETP Lett.* **57**, 69 (1993).
- <sup>7</sup>G. L. Yuan, S. W. Or, and H. L. W. Chan, *J. Phys. D* **40**, 1196 (2007).
- <sup>8</sup>D. H. Wang, W. C. Goh, M. Ning, and C. H. Ong, *Appl. Phys. Lett.* **88**, 212907 (2006).
- <sup>9</sup>Y. Wang and C. W. Nan, *Appl. Phys. Lett.* **89**, 052903 (2006).
- <sup>10</sup>S. T. Zhang, Y. Zhang, M. H. Lu, C. L. Du, Y. F. Chen, Z. G. Liu, Y. Y. Zhu, and N. B. Ming, *Appl. Phys. Lett.* **88**, 162901 (2006).
- <sup>11</sup>G. L. Yuan, S. W. Or, J. M. Liu, and Z. G. Liu, *Appl. Phys. Lett.* **89**, 052905 (2006).
- <sup>12</sup>A. V. Zaleskii, A. A. Frolov, T. A. Khimich, and A. A. Bush, *Phys. Solid State* **45**, 141 (2003).
- <sup>13</sup>Y. H. Lin, Q. H. Jiang, Y. Wang, and C. W. Nan, *Appl. Phys. Lett.* **90**, 172507 (2007).
- <sup>14</sup>C. C. Lee and J. M. Wu, *Electrochem. Solid-State Lett.* **10**, G58 (2007).
- <sup>15</sup>J. G. Wu and J. Wang, *J. Am. Ceram. Soc.* **93**, 8 (2010).
- <sup>16</sup>G. Le Bras, D. Colson, A. Forget, N. Genand-Riondet, R. Tourbot, and P. Bonville, *Phys. Rev. B* **80**, 134417 (2009).
- <sup>17</sup>Y. P. Wang, L. Zhou, M. F. Zhang, X. Y. Chen, J. M. Liu, and Z. G. Liu, *Appl. Phys. Lett.* **84**, 1731 (2004).
- <sup>18</sup>S. Kamba, D. Nuzhnyy, M. Savino, J. Šěbek, J. Petzelt, J. Proklečka, R. Haumont, and J. Kreisel, *Phys. Rev. B* **75**, 024403 (2007).
- <sup>19</sup>G. Catalan, *Appl. Phys. Lett.* **88**, 102902 (2006).